International Journal of Applied Engineering Research ISSN 0973-4562 Volume 12, Number 22 (2017) pp.12415-12420

Hot Deformation Characteristics of 304 Stainless Steels by Tensile Test

JongHun Kang[1], JaeUk Yoo [2], KuHee Ann [3], YongChul Kwon[4#]

[1]*Department of Mechatronics Engineering, Jungwon University, Chungbuk,, South Korea.*
[2]*Material and Component Service Center, Gyeongnam Technopark, Gyeongnam,, South Korea.*
[3]*R&D Center, Taejung Co., Chungbuk,, South Korea.*
[4]*Yeungnam Advanced Business Division, Korea Conformity Laboratories, Busan, South Korea.*

Abstract

Hot flow characteristics are important parameters in the analysis of a large deformation process by finite element method. Hot flow stress is generally calculated by a compression test in which the calculation may produce errors due to the friction between the test jig and the tested material. In the present study, a hydraulic Gleeble machine was used to perform a high-temperature tensile test with S304, an austenite stainless steel. The strain rate was set at 1, 5, and 10 mm/mm sec in the test; the test interval was 100℃ in a range from 800℃ to 1200℃. The flow stress was calculated by the inverse method with the measured displacement and load data. For the flow stress model obtained by the calculation, the model parameters were calculated using the Hansel-Spittel model as a forge. The analysis and the test work of M24 Nut hot forming were carried out, and the validity of the obtained flow stress was verified through the analogy of the forging and the flow pattern from the finite element analysis.

Keywords: Flow Stress, Hansel-Spittel model, Hot working, Tensile Test, S304

INTRODUCTION

In hot forming processes, including rolling, forging, drawing, and extrusion, the flow stress is affected by the strain, strain rate, and temperature of the raw material. Therefore, studies have been conducted with various materials and test conditions to calculate the flow stress by using the strain and load curve obtained experimentally under isothermal and constant strain rate conditions. Hot deformation accompanies recovery and recrystallization, wherein the flow stress reaches a peak and then decreases in a material having a strong recrystallization tendency. Spittel et al.(1978) suggested a flow stress equation for the strain, and a strain rate sensitivity coefficient using the temperature, strain, strain rate, and peak strain, as shown in Equation (1):

$$\bar{\sigma} = A_1 \exp(m_1 T)(\varepsilon + \varepsilon_0)^{m_2} \exp\left(\frac{m_4}{(\varepsilon + \varepsilon_0)}\right) \exp(m_7(\varepsilon + \varepsilon_0)) \quad (1)$$

Horsinka et al., and Opela et al. determined a flow stress model for aluminum alloys and C45 steel using the Hansel-Spittel equation. Since hot flow stress is affected by strain, strain rate, and temperature, Moon et al. expressed the flow stress in terms of the strain rate and the strain rate sensitivity coefficient, representing the strain rate sensitivity coefficient as a function of the strain and the temperature; they then calculated the flow stress using the inverse method of finite element analysis

$$\bar{\sigma} = A_1 \dot{\varepsilon}^{m_3(C,T)} \quad (2)$$

Meyer summarized models that may represent cold and hot flow stress and compared the pros and cons of the models [5].

The flow stress model mentioned above focuses on the expression of the macroscopic behavior of a material depending on the strain, strain rate, and temperature. However, due to the strain energy, the hot deformation process softens a material through continued recrystallization and recovery. Therefore, a flow stress model needs to predict recrystallization and recovery phenomena. Sellars et al. and Rao et al., by using the activation energy and the Zener Holloman parameter, suggested a flow stress model considering the microstructural evolution:

$$\dot{\varepsilon} = A \sinh(\alpha\sigma)^n \exp(-\frac{Q}{RT}) \quad (3)$$

Where A and α are constant, n is related to strain sensitivity, Q is activation energy of deformation, R is the gas constant, and T is the absolute temperature. Equation (3) can be expressed with ZenerHolloman parameter

$$Z = \dot{\varepsilon} \cdot \exp(\frac{Q}{RT}) \quad (4)$$

$$Z = A \sinh(\alpha\sigma)^n \quad (5)$$

The studies were extended to the prediction of microstructural evolution by defining the critical strain of dynamic recrystallization onset with the Zener Holloman parameter of Equation (5), the stress, and the work hardening rate [9-11]. In addition, the scope of the study was extended to the development of a deformation processing map in which the workability may be determined by the temperature, strain, and strain rate in Equation (5) [12-16].

In the present study, the conventional hot flow stress equation was obtained by performing a compression test. However, to minimize the effect of the compression test jig, the load and deformation data were obtained using tensile test specimens at strain rates of 1, 5, and 10/s in a temperature range between 800℃ and 1200℃. Variations of the tensile strength and the elongation rate depending on the temperature and the strain rate were analyzed using the test results. In addition, flow stress considering necking, which depends on the test conditions, was analyzed by the inverse method using the Forge software.

TENSILE TEST

A tensile test to obtain the hot flow stress was performed using the Gleeble equipment. Figure 1 shows the dimensions of the tensile test specimens.

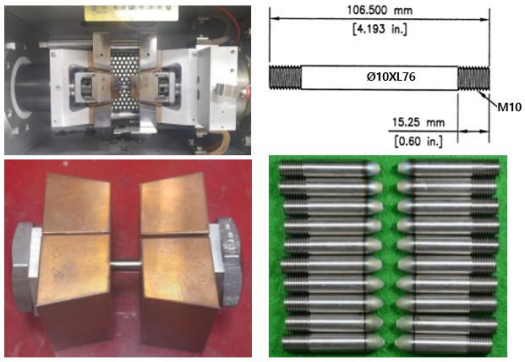

Figure 1: Jig setup and specimens for tensile test

The hot tensile test specimens were processed using austenite stainless steel and SUS304 materials according to the dimensions shown in Figure 1. The tensile test was performed at strain rates of 1, 5, and 10/s by heating the specimens to 800℃, 900℃, 1000℃, 1100℃, and 1200℃. Figure 2 shows the load-displacement curve obtained by the tensile test.

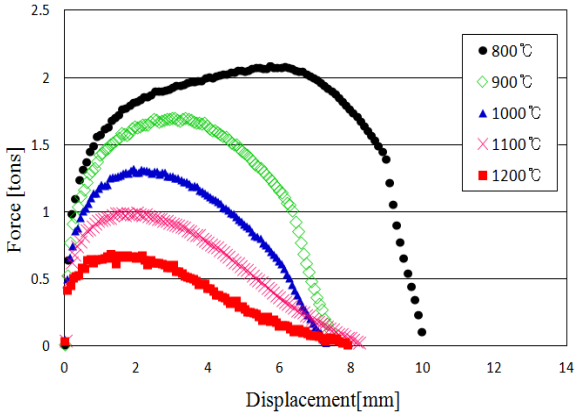

(a) Strain rate 1/s

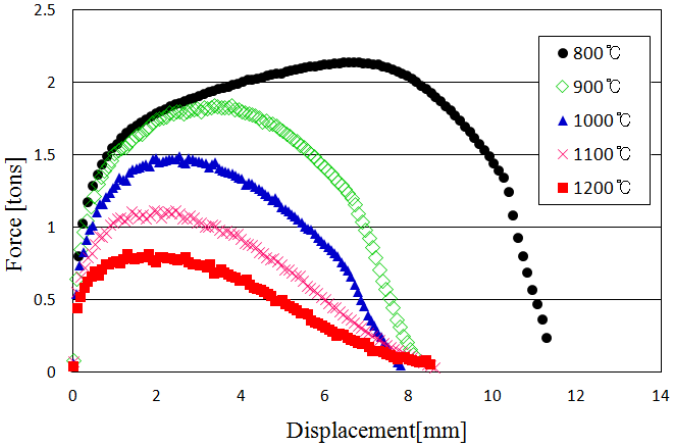

(b) Strain rate 5/s

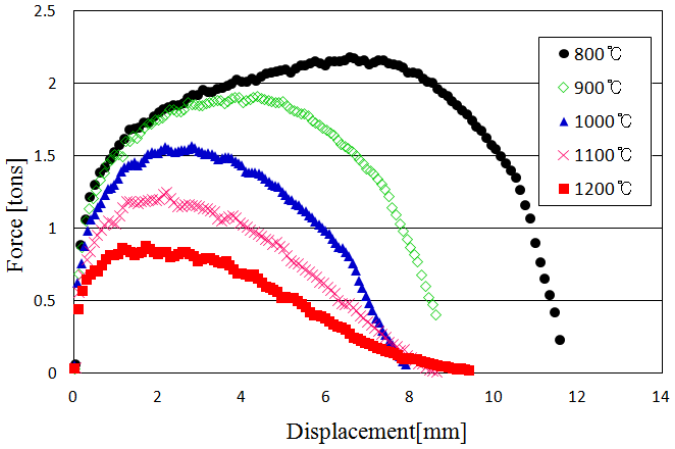

(c) Strain rate 10/s

Figure 2: Force – displacement data from tensile test

The analysis of the maximum tensile strength and the maximum yield strength of SUS 304 depending on the strain rate and temperature showed that the strength increased with increasing strain rate and with decreasing temperature, as shown in Figure 3.

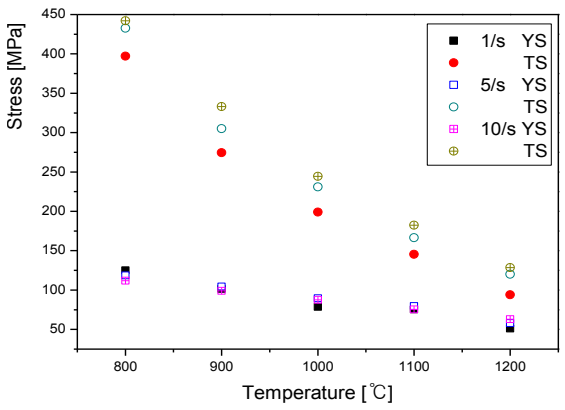

Figure 3: Analysis results of TS and YS according to strain rate

Generally, the elongation rate of steel materials decreases as the strength increases. However, at the strain rate of 1/s, the elongation rates of SUS 304 were 60% at 800℃, 48.5% at 900℃, 46% at 1000℃, and 51.5% at 1100℃, indicating that the elongation rate and the strength increased with decreasing temperature. In addition, the analysis of the elongation rate at 800℃ depending on the strain rate showed that the elongation rates were 60% at 1/s, 66.5% at 5/s, and 67.5% at 10/s. This indicates that the toughness increased with the increase of the strain rate, as shown in Figure 4.

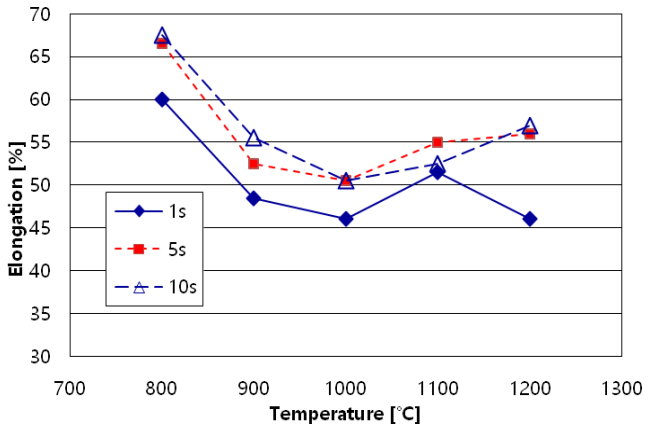

Figure 4: Elongation comparison according to test conditions

HOT FLOW STRESS MODEL

The hot flow stress equation employed in the present study was the Hansel-Spittel equation, shown in Equation (1). The parameters of Equation (1) were calculated through repeated analyses using the load and displacement values obtained from the experiment through the inverse method in the Forge NX software. The parameters in Equation (1) were calculated for each of the test temperatures. Table 1 shows the calculated parameters

Table 1: arameter calculation result by inverse method

Temp.	A1	m2	m4	m7
800℃	2730	0.793	0.00864	-0.944
900℃	2290	0.687	0.0081	-1.2
1000℃	2090	0.652	0.00744	-1.65
1100℃	1720	0.629	0.00648	-1.83
1200℃	1125.4	0.558	0.006907	-2.1

The individual parameters for Equation (1) were calculated for each of the test temperatures. Figure 5 shows the plots of the parameters obtained at each temperature.

As can be seen from the plots in Figure 5, each of the parameters showed linear variation depending on the temperature. These variations may be approximated by the linear equations from Equation (6) to (10).

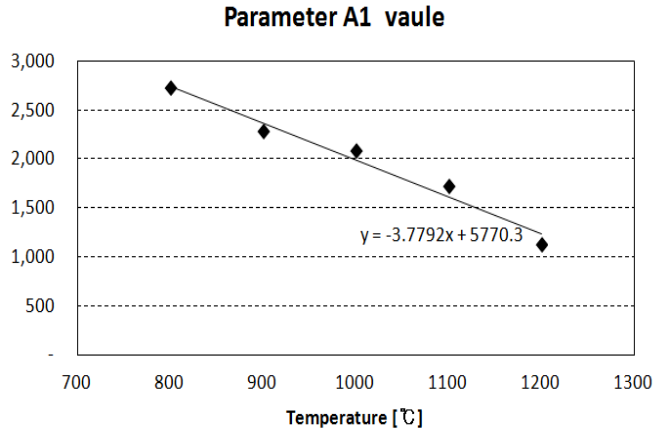

(a) Parameter A1

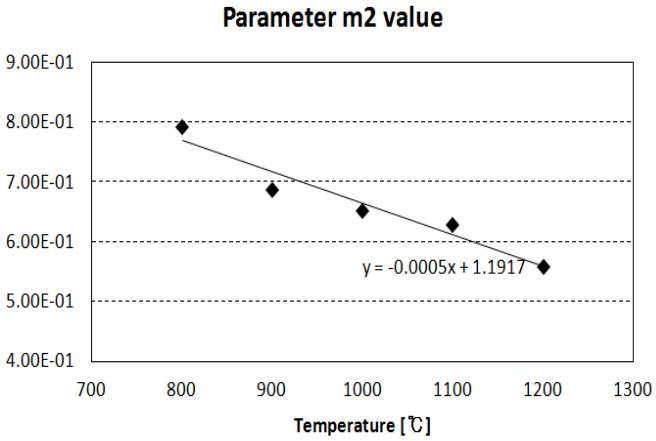

(b) Parameter m2

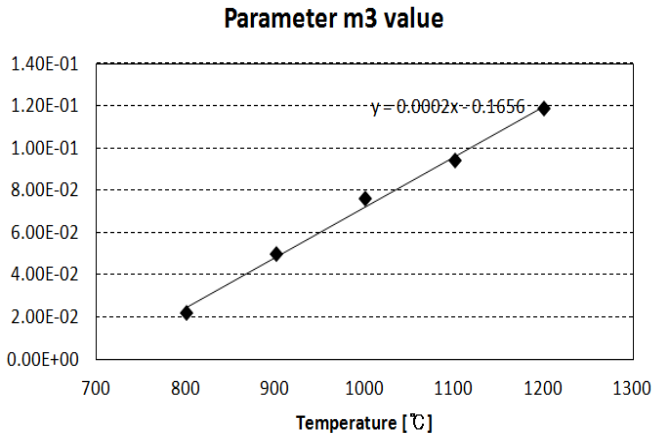

(c) Parameter m3

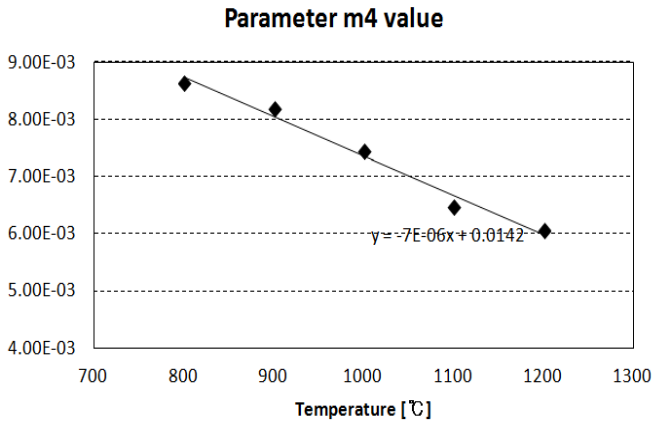

(d) Parameter m4

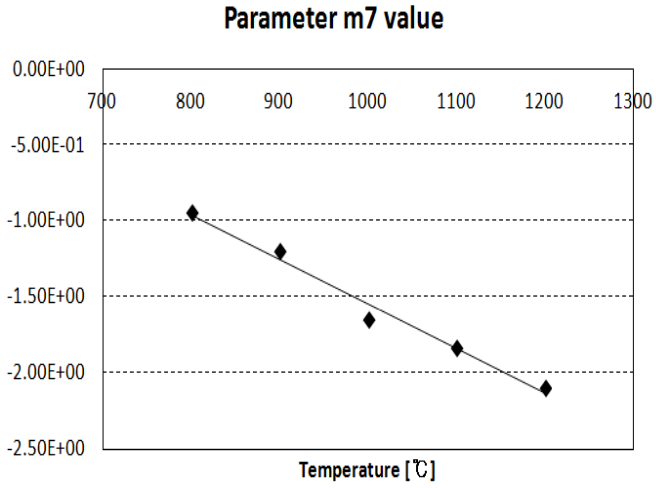

(e) Parameter m7

Figure 5: Parameter value by inverse method

$$A_1 = -3.7792T + 5770.3 \quad (6)$$

$$m_2 = -0.0005T + 1.1917 \quad (7)$$

$$m_3 = 0.0002T - 0.1656 \quad (8)$$

$$m_4 = -7x10^{-6}T + 0.0142 \quad (9)$$

$$m_7 = -0.0029T + 1.3972 \quad (10)$$

The flow stress depending on the strain at different temperatures and strain rates was calculated by substituting Equations (6) to (10) into Equation (1), entering the strain rates of 1, 5, and 10/s and the temperature values of 800, 900, 1000, 1100, and 1200℃, and infinitesimally increasing the strain rate. Figure 6 shows the plots of the calculated flow stress.

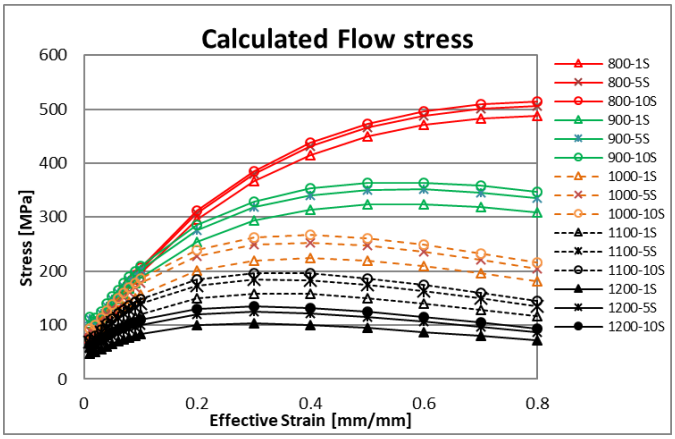

Figure 6: True strain – stress curve calculated by inverse method

TENSILE ANALYSIS WITH CALCULATED FLOW STRESS

Finite element analysis was performed using the flow stress of SUS304, shown in Figure 6, under the same conditions as those of the tensile test. Finite element analysis was performed using the Forge NX software. The analysis was performed under the same strain rate and temperature conditions as those of the tensile test.

Figure 8 provides images of the specimens and the finite element analysis results before and after the tensile test.

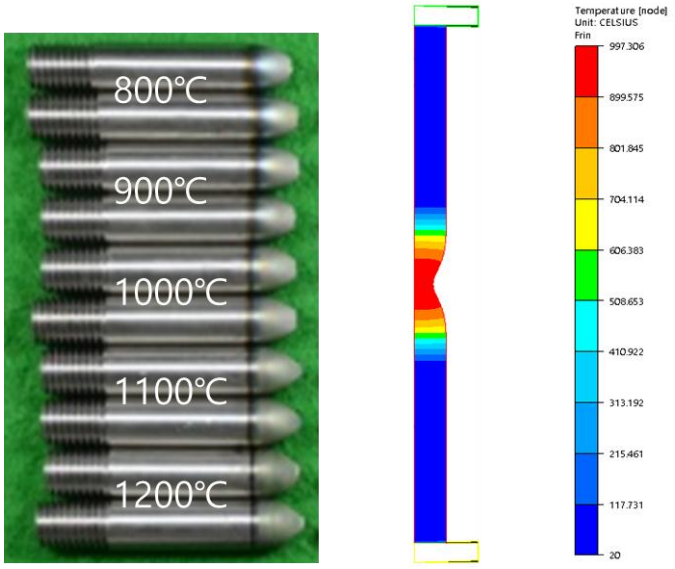

Figure 7: Neck shape comparison between test and analysis

The displacement and load may be calculated through finite element analysis of the tensile test results. Figure 7 shows the load-displacement curves at different temperature values, obtained by finite element analysis and the tensile test that were carried out under the same conditions.

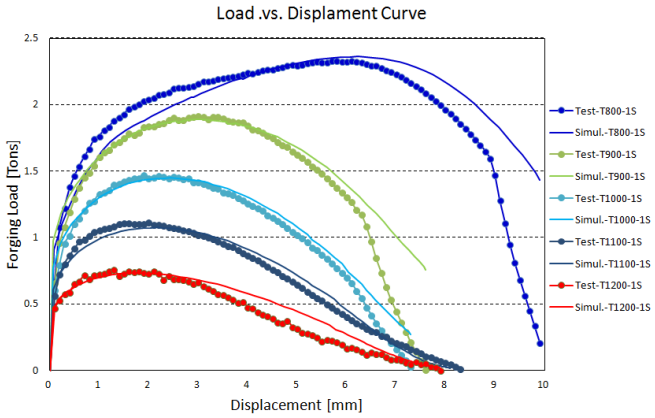

(a) strain rate 1/s

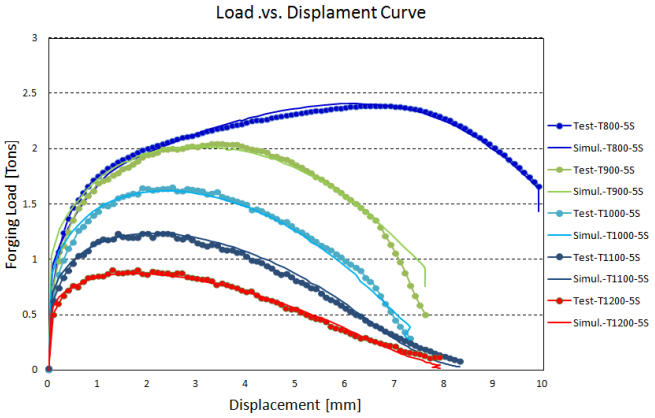

(b) strain rate 5/s

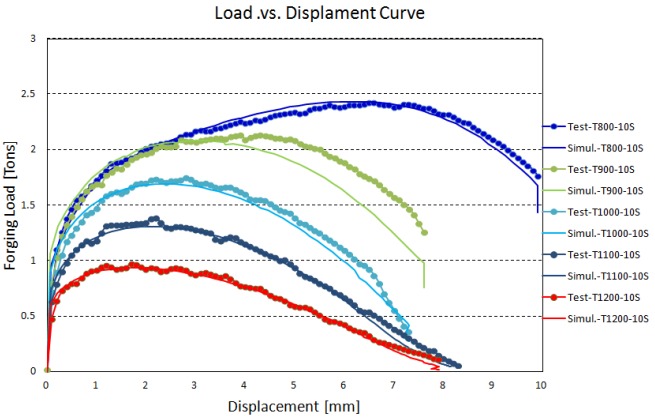

(c) strain rate 1/s

Figure 8: Comparison of forging load between measurements and finite element analysis results

FORGING ANALYSIS WITH ACQUIRED FLOW STRESS

The results of an actual M24 bolt forming process and of the finite element analysis were compared using the flow stress obtained by the tensile test. The finite element analysis was performed using a 36,000-mesh and a 1/6 model. The velocity at each punch position was given by considering the Ram movement chart and the operation speed (95SPM) of the equipment.

SUS304, showing the best elongation rate at 800℃, may have advantages against material cracks, but the increase of the flow stress with increasing temperature could cause fatal damage to the mold. Therefore, finite element analysis was performed at the heating temperature of 1200℃. Figure 9 compares the finite element analysis results with the forming test results. The forging test results also showed chamfer at the extruding inlet in the back and an unfilled shape at the external hexagonal part of the nut.

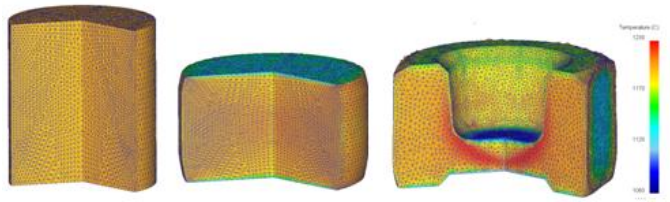

(a) Finte element results

(b) Forging test results

Figure 9: Forging analysis and test results

CONCLUSION

To calculate the flow stress of SUS304, which is a representative material that is difficult to form, a tensile test and a numerical analysis were performed in a temperature range allowing hot forming, between 800 and 1200℃, and at strain rates of 1, 5, and 10/s.

(1) The yield strength was found to be not significantly dependent on the strain rates of 1, 5, and 10/s, while the tensile strength was significantly dependent on the strain rate.

(2) The ratio of cross-sectional area decrease was highest at 800℃ and 10/s, but it decreased up to 1000℃ and then increased again with increasing temperature. In view of the strength and the cross-sectional area decrease rate, a higher temperature than 1100℃ may be considered as an appropriate forging temperature.

(3) The flow stress was calculated using the measured load-displacement data through the inverse method in the Hansel-Spittel model. Through the calculation of the flow stress, the

load-displacement data were compared between the test and the analysis to verify the accuracy of the model.

(4) Finite element analysis was performed using the calculated flow stress; a forging test was also performed. The shape of the actual forged product was consistent with the predictions of the finite element method, verifying that flow stress may be calculated using the tensile stress.

ACKNOWLEDGEMENT

This work was supported by the Technology Innovation Program (No.: 10067300, "Development of forming technology for high corrosion resistant and heat-resistant fasteners with a hard forming material.") funded By the Ministry of Trade, industry & Energy (MI, Korea)

REFERENCES

[1] T.Spittel, A.Hensel, Krafts und Arbeisbedarf bildsamer Formgebungsverfahren, Leipyig, VEB, 978, 528s.

[2] J.Horsinka, J.Kliber, K. Drozd, I.Mamuzic, 2011, Approximation model of the stress-strain curve for deformation of aluminum alloys, METABK, 50(2), 81-84.

[3] P.Opela, I.Schindler, P.Kawulok, F.Vandura, R.Kawulok, S.Rusz, T.Petrek, 2015, Hot flow stress models of the steel C45, Metabk, 54(3), 469-472.

[4] H.K. Moon, J.S. Lee, S.J Yoo, M.S. Joun and J.K. Lee, 2007, Hot Deformation Behavior of Bearing Steels, Journal of Engineering Material Technology, 129(3) 349-355.

[5] L.W.Meyer, A.Weise and F.Hahn, 1997, Comparison of Constitutive Flow Curve Relations in Cold and Hot Forming, Journal of Physics IV France 7, C3,13~20.

[6] C.M Sellars and W.J.M. Tegart, 1972, Hot workability, International Material Reviews, 17, 1-24.

[7] K.P. Rao, Y.K.D.V. Parasad and E.B. Hawbolt, 1996, Hot deformation studies on a low-carbon steel: part1 – Flow curves and the constitutive relationship, Journal of Material Processing Technology, 56, 897-907.

[8] K.P. Rao, Y.K.D.V. Parasad and E.B. Hawbolt, 1996, Hot deformation studies on a low-carbon steel: part2 – An algorithm for the flow stress determination under varying process conditions, Journal of Material Processing Technology, 56, 908-917.

[9] S. Solhjoo, 2010, Determination of critical strain for initiation of dynamic recrystallization, Materials and Design, 31, 1360–1364.

[10] D.N. Zou, K.Wu, Y. Han, W. Zhang, B. Cheng and G.J. Qiao, 2013, Deformation characteristic and prediction of flow stress for as-cast 21Cr economical duplex stainless steel under hot compression, Materials and Design, 51, 975–982.

[11] S.V. Mehtonen, L.P. Karjalainen, and D.A. Porter, 2014, Modeling of the high temperature flow behavior of stabilized 12–27 wt% Cr ferritic stainless steels, Materials Science & Engineering A, 607, 44–52.

[12] S. Venugopal, S. Venugopal, P.V. Sivaprasad, M. Vasudevan, S.L. Mannan, S.K. Jha, P. Pandey and Y.V.R.K. Prasad, 1995, Validation of processing maps for 304L stainless steel using hot forging, rolling and extrusion, Journal of Materials Processing Technology, 59, 343 – 350.

[13] A.Momeni and K. Dehghani, 2011, Hot working behavior of 2205 austenite–ferrite duplex stainless steel characterized by constitutive equations and processing maps, Materials Science and Engineering A, 528, 1448–1454.

[14] H. Sun, Y. Sun, R. Zhang, M. Wang, R. Tang and Z. Zhou, Study on hot workability and optimization of process parameters of a modified 310 austenitic stainless steel using processing maps, Materials and Design, 67, 165–172.

[15] D. Barbier, J.D. Guérin, M. Dubar, T. Bénard, S.Bonneau and E.S. P. Cabrera, 2017, Hot ductility and flow stress of AISI 4130 and 52100-type steels, Materials Science & Engineering A, 690, 37–43.

[16] K.A. Babu, S. Mandal, C.N. Athreya, B. Shakthipriya and V.S. Sarma, 2017, Hot deformation characteristics and Processing map of a phosphorous modified super austenitic stainless steel, Materials and Design, 115 , 262–275.